

The effects of combining alloying elements on the elastic properties of *γ* -Ni in Ni-based superalloy: High-throughput first-principles calculations

Baokun Lu(路宝坤), Chongyu Wang(王崇愚)

Citation: Chin. Phys. B . 2018, 27(7): 077104. **doi:** 10.1088/1674-1056/27/7/077104

Journal homepage: http://cpb.iphy.ac.cn; http://iopscience.iop.org/cpb

What follows is a list of articles you may be interested in

Magnetic interactions in a proposed diluted magnetic semiconductor $(Ba_{1-x}K_x)(Zn_{1-y}Mn_y)_2P_2$

Huan-Cheng Yang(杨焕成), Kai Liu(刘 凯), Zhong-Yi Lu(卢仲毅)

Chin. Phys. B . 2018, 27(6): 067103. **doi:** 10.1088/1674-1056/27/6/067103

First-principles investigations of proton generation in *α*-quartz

Yunliang Yue(乐云亮), Yu Song(宋宇), Xu Zuo(左旭)

Chin. Phys. B . 2018, 27(3): 037102. **doi:** 10.1088/1674-1056/27/3/037102

Electronic and mechanical properties of half-metallic half-Heusler compounds CoCr*Z* (*Z*=S, Se, and Te)

Hai-Ming Huang(黄海铭), Chuan-Kun Zhang(张传坤), Ze-Dong He(贺泽东), Jun Zhang(张俊), Jun-Tao Yang(杨俊涛), Shi-Jun Luo(罗时军)

Chin. Phys. B . 2018, 27(1): 017103. **doi:** 10.1088/1674-1056/27/1/017103

First-principles study of helium clustering at initial stage in ThO_2

Kuan Shao(邵宽), Han Han(韩晗), Wei Zhang(张伟), Chang-Ying Wang(王昌英), Yong-Liang Guo(郭永亮), Cui-Lan Ren(任翠兰), Ping Huai(怀平)

Chin. Phys. B . 2017, 26(9): 097101. **doi:** 10.1088/1674-1056/26/9/097101

Optical properties of anatase and rutile TiO_2 studied by GGA+*U*

Jinping Li(李金平), Songhe Meng(孟松鹤), Liyuan Qin(秦丽媛), Hantao Lu(陆汉涛)

Chin. Phys. B . 2017, 26(8): 087101. **doi:** 10.1088/1674-1056/26/8/087101

The effects of combining alloying elements on the elastic properties of γ-Ni in Ni-based superalloy: High-throughput first-principles calculations*

Baokun Lu(路宝坤) and Chongyu Wang(王崇愚)†

Department of Physics, Tsinghua University, Beijing 100084, *China*

(Received 17 June 2018; published online 25 June 2018)

Using high-throughput first-principles calculations, we systematically studied the synergistic effect of alloying two elements (Al and 28 kinds of 3d, 4d, and 5d transition metals) on the elastic constants and elastic moduli of γ-Ni. We used machine learning to theoretically predict the relationship between alloying concentration and mechanical properties, giving the binding energy between the two elements. We found that the ternary alloying elements strengthened the γ phase in the order of Re > Ir > W > Ru > Cr > Mo > Pt > Ta > Co. There is a quadratic parabolic relationship between the number of d shell electrons in the alloying element and the bulk modulus, and the maximum bulk modulus appears when the d shell is half full. We found a linear relationship between bulk modulus and alloying concentration over a certain alloying range. Using linear regression, we found the linear fit concentration coefficient of 29 elements. Using machine learning to theoretically predict the bulk modulus and lattice constants of $Ni_{32}XY$, we predicted values close to the calculated results, with a regression parameter of $R^2 = 0.99626$. Compared with pure Ni, the alloyed Ni has higher bulk modulus B, G, E, C_{11}, and C_{44}, but equal C_{12}. The alloying strengthening in some of these systems is closely tied to the binding of elements, indicating that the binding energy of the alloy is a way to assess its elastic properties.

Keywords: Ni-based single crystal superalloy, high-throughput calculations, first-principles calculations, elastic properties

PACS: 71.20.Be, 81.05.Bx, 31.15.es **DOI:** 10.1088/1674-1056/27/7/077104

1. Introduction

Ni-based single-crystal (SC) superalloys are widely used in turbine blades in aircraft jet engines and land-based power generators because they have excellent high-temperature properties, including strength, ductility, fracture toughness, and fatigue resistance, as well as enhanced creep and oxidation resistance.[1] To increase their lifetime and service temperature, Ni-based superalloys are often alloyed with ten or more elements, making them some of the most complex alloys.

The elastic moduli of a material can be used to assess its mechanical properties such as ductility and brittleness, hardness, and strength. The bulk modulus (B) represents a material's average resistance to bond breakage, and its shear modulus (G) is closely linked to its resistance to plastic deformation. Furthermore, the B/G ratio of a metal is related to its ductility, as proposed by Pugh:[2] a material with a large B/G ratio (> 1.75) will show ductile behavior, while one with a low B/G ratio (< 1.75) will show brittle behavior. To understand and develop next-generation Ni-based superalloys, we must systematically study their fundamental properties and show how alloying elements affect their mechanical properties.

In this paper, we study how alloying transition metals from three periods, i.e., 3d (Sc, Ti, V, Cr, Mn, Fe, Co, Ni, Cu, Zn), 4d (Y, Zr, Nb, Mo, Tc, Ru, Rh, Pd, Ag, Cd), and 5d (Hf, Ta, W, Re, Os, Ir, Pt, Au), affect the elastic properties in Ni dilute solid solutions, using first-principles calculations with the efficient stress–strain method.

2. Computational methods

2.1. First-principles calculations

We performed *ab initio* total-energy calculations with Vienna *ab initio* simulation package (VASP) code[3–6] based on density functional theory. The pseudo-potentials used to describe the interactions between nuclear and extranuclear electrons were obtained using the projector augmented wave (PAW) method.[7] The electronic exchange–correlation energy was treated within the generalized gradient approximation (GGA) with the Perdew–Burke–Ernzerhof functional.[8] The plane wave kinetic energy cut-off was set to 350 eV to ensure total energy convergence to 10^{-5} eV and force convergence to -0.02 eV/Å. The integration over the Brillouin zone (BZ) was done using a Monkhorst–Pack grid.[9] For accurate calculations of total energy, we used a $11 \times 11 \times 11$ k-point sampling grid for 32-atom supercells and a $5 \times 5 \times 5$ k-point sampling grid for 108-atom supercells.

2.2. Method of calculating elastic properties

The elastic behavior of a completely asymmetric material is specified by 21 independent elastic constants, while that of an isotropic material is specified by 2. Between these limits, the number of constants depends on the symmetry of the ma-

*Project support by the National Key R&D Program of China (Grant Nos. 2017YFB0701501, 2017YFB0701502, and 2017YFB0701503).

†Corresponding author. E-mail: cywang@mail.tsinghua.edu.cn

© 2018 Chinese Physical Society and IOP Publishing Ltd

terial.

For the tetragonal structure $a = b \neq c$, $\alpha = \beta = \gamma = 90^\circ$, $C_{11} = C_{22}$, $C_{13} = C_{23}$, and $C_{44} = C_{55}$. Tetragonal crystals require 6 constants, usually referred to as C_{11}, C_{33}, C_{44}, C_{66}, C_{12}, and C_{13}, as shown in Eq. (1). Thus, theoretically estimating the elasticity for a tetragonal system is much more involved than for a cubic system, which only has three constants (C_{11}, C_{12}, and C_{44}). For the cubic structure $a = b = c$, $\alpha = \beta = \gamma = 90^\circ$, $C_{11} = C_{22} = C_{33}$, $C_{12} = C_{13} = C_{23}$, and $C_{44} = C_{55} = C_{66}$.

$$\{C_{ij}\} = \begin{pmatrix} C_{11} & C_{12} & C_{13} & 0 & 0 & 0 \\ C_{12} & C_{11} & C_{13} & 0 & 0 & 0 \\ C_{13} & C_{13} & C_{33} & 0 & 0 & 0 \\ 0 & 0 & 0 & C_{44} & 0 & 0 \\ 0 & 0 & 0 & 0 & C_{44} & 0 \\ 0 & 0 & 0 & 0 & 0 & C_{66} \end{pmatrix}. \quad (1)$$

Elastic constants are defined by a Taylor expansion of the total energy $E(V,e)$. For a small strain ε, we can use Hooke's law to approximate the elastic energy E by a quadratic function of the strain components

$$E(V,e) = E(V_0,0) + V_0\left(\sum_{i=1}^{6}\tau_i e_i + \frac{1}{2}\sum_{i=1}^{6}\sum_{j=1}^{6} C_{ij}e_i e_j + O(e^3)\right), \quad (2)$$

where C_{ij} are the elastic constants, V_0 is the equilibrium volume of the unit cell, and e_i is the component of the strain tensor ε, which can be related to the deformation tensor $\boldsymbol{D}$ as

$$\varepsilon = \boldsymbol{D} - \boldsymbol{I} = \frac{1}{2}\begin{pmatrix} 2e_1 & e_6 & e_5 \\ e_6 & 2e_2 & e_4 \\ e_5 & e_4 & 2e_3 \end{pmatrix}. \quad (3)$$

This is written in conventional elastic theory notation (where $\boldsymbol{I}$ represents the identity matrix). To determine these six independent elastic constants of tetragonal crystals, we need six strains. The six distortions used in the tetragonal crystal are described as Table 1.

Table 1. Components of the strain tensor for a tetragonal system [$u = (1-\delta^2)^{-1/2}$].

e_1	e_2	e_3	e_4	e_5	e_6	$E(V,\delta)$
δ	0	0	0	0	0	$E(V,\delta) = E(V_0,0) + V_0(\tau_1\delta + \frac{C_{11}}{2}\delta^2)$
0		0δ	0	0	0	$E(V,\delta) = E(V_0,0) + V_0(\tau_3\delta + \frac{C_{33}}{2}\delta^2)$
0	0	0	02δ	0	0	$E(V,\delta) = E(V_0,0) + V_0(2\tau_4\delta + 2C_{44}\delta^2)$
0	0	0	0	0	2δ	$E(V,\delta) = E(V_0,0) + V_0(2\tau_6\delta + 2C_{66}\delta^2)$
$u(1+\delta)-1$	$u(1-\delta)-1$	$u-1$	0	0	0	$E(V,\delta) = E(V_0,0) + V_0[(\tau_1-\tau_2)\delta + (C_{11}-C_{22})\delta^2]$
$u(1+\delta)-1$	$u-1$	$u(1-\delta)-1$	0	0	0	$E(V,\delta) = E(V_0,0) + V_0[(\tau_1-\tau_3)\delta + \frac{1}{2}(C_{11}+C_{33}-2C_{13})\delta^2]$

Because cubic symmetry is disrupted by alloying atoms, we estimated the average elastic constants for each configuration as

$$\overline{C}_{11} = \frac{2C_{11}+C_{33}}{3},$$
$$\overline{C}_{44} = \frac{2C_{44}+C_{66}}{3},$$
$$\overline{C}_{12} = \frac{C_{12}+2C_{13}}{3}. \quad (4)$$

In both the Voigt average[10] and Reuss average,[11] the polycrystalline results are determined from the elastic constants. For a tetragonal lattice, the Reuss shear modulus G_{R} and the Voigt shear modulus G_{V} are

$$G_{\mathrm{R}} = \frac{15}{4(2S_{11}+S_{33}-4(S_{12}+2S_{13})+3(2S_{44}+S_{66}))},$$
$$G_{\mathrm{V}} = \frac{1}{15}(2C_{11}+C_{33}-C_{12}-2C_{13}+6C_{44}+3C_{66}), \quad (5)$$

and the Reuss bulk modulus (B_{R}) and the Voigt bulk modulus (B_{V}) are defined as

$$B_{\mathrm{R}} = \frac{1}{2S_{11}+S_{33}+2S_{12}+4S_{13}},$$
$$B_{\mathrm{V}} = \frac{1}{9}(2C_{11}+C_{33}+2C_{12}+4C_{13}), \quad (6)$$

where $\boldsymbol{S}$ is the compliance matrix and $\boldsymbol{C}$ is the elastic constant matrix, related by $\boldsymbol{S} = \boldsymbol{C}^{-1}$. For a tetragonal crystal, the compliance matrix $\boldsymbol{S}$ can be expressed by

$$\{S_{\mathrm{ij}}\} = \begin{pmatrix} S_{11} & S12 & S_{13} & 0 & 0 & 0 \\ S_{12} & S11 & S_{13} & 0 & 0 & 0 \\ S_{13} & S13 & S_{33} & 0 & 0 & 0 \\ 0 & 0 & 0 & S_{44} & 0 & 0 \\ 0 & 0 & 0 & 0 & S_{44} & 0 \\ 0 & 0 & 0 & 0 & 0 & S_{66} \end{pmatrix}, \quad (7)$$

where

$$S_{11} = \frac{C_{13}{}^2 - C_{11}C_{33}}{C_{33}C_{12}{}^2 + 2C_{11}C_{13}{}^2 - 2C_{12}C_{13}{}^2 - C_{33}C_{21}^2},$$
$$S_{33} = \frac{C_{11} + C_{12}}{C_{33}C_{12}{}^2 + C_{11}C_{33} - 2C_{13}},$$
$$S_{12} = \frac{C_{12}C_{33} - C_{13}{}^2}{C_{33}C_{12}^2 + C_{11}C_{13}^2 - 2C_{12}C_{13}^2 - C_{33}C_{11}^2},$$
$$S_{13} = \frac{C_{13}}{2C_{13}^2 - C_{33}C_{12} - C_{33}C_{11}},$$
$$S_{44} = \frac{1}{C_{44}}, \quad S_{66} = \frac{1}{C_{66}}. \tag{8}$$

Using energy considerations, Hill[12] proved that the Voigt and Reuss equations represent the upper and lower limits of the true polycrystalline constants, and recommended that practical estimates of the bulk and shear moduli are the arithmetic means of these extremes. Hence, the elastic moduli of a polycrystalline material can be approximated by Hill's average, which for shear moduli is

$$B_{\mathrm{H}} = \frac{B_{\mathrm{V}} + B_{\mathrm{R}}}{2},$$
$$G_{\mathrm{H}} = \frac{G_{\mathrm{V}} + G_{\mathrm{R}}}{2}. \tag{9}$$

The Young's modulus (E) and Poisson's ratio (υ) of an isotropic material are given by

$$E = \frac{9B_{\mathrm{H}}G_{\mathrm{H}}}{3B_{\mathrm{H}} + G_{\mathrm{H}}},$$
$$\upsilon = \frac{3B_{\mathrm{H}} - 2G_{\mathrm{H}}}{2(3B_{\mathrm{H}} + G_{\mathrm{H}})}. \tag{10}$$

Based on these relations, Table 2 gives the calculated bulk modulus (B), shear modulus (G), Young's modulus (E), and Poisson's ratio (υ) for $Ni_{31}X$.

3. Results and discussion

3.1. Mechanical properties of single-element alloying

Table 2 summarizes the calculated elastic properties of the $Ni_{31}X$ alloys. The calculated bulk properties of γ-Ni agree well with reported measurements, the calculated C_{ij}'s of fcc Ni agree well with reported measurements, and the calculated elastic properties of fcc Ni agree well with reported first-principles calculations.[13–19]

Table 2. Elastic constants and moduli of the $Ni_{31}X$ system.

Element	B/GPa	C_{11}/GPa	C_{12}/GPa	C_{44}/GPa	G/Gpa	E/GPa
Al	194.04	248.40	166.86	114.32	75.65	200.85
Sc	187.38	236.51	162.81	102.23	67.94	181.83
Ti	194.76	247.80	168.25	110.57	73.42	195.67
V	197.63	253.47	169.71	117.38	77.69	206.06
Cr	198.98	256.84	170.04‘	121.21	80.34	212.42
Mn	199.09	256.17	170.55	117.80	78.53	208.22
Fe	198.69	254.27	170.89	116.29	77.11	204.84
Co	197.82	250.68	171.39	112.60	74.14	197.71
Ni	196.41	246.88	171.17	109.82	71.71	191.79
Cu	194.34	244.91	169.05	111.96	72.61	193.70
Zn	192.96	244.85	167.02	110.66	72.83	194.06
Y	180.01	225.39	157.32	95.38	63.13	169.57
Zr	190.32	239.64	165.66	104.53	68.96	184.58
Nb	196.04	248.80	169.66	111.49	73.64	196.34
Mo	198.95	254.20	171.32	116.01	76.82	204.18
Tc	199.80	256.05	171.67	116.49	77.56	206.01
Ru	199.40	255.21	171.50	116.55	77.34	205.46
Rh	197.79	250.70	171.34	112.25	74.02	197.44
Pd	194.84	244.13	170.19	107.28	70.05	187.65
Ag	190.63	238.04	166.92	106.00	68.49	183.49
Cd	188.43	236.67	164.32	107.51	69.54	185.77
Hf	192.07	242.61	166.81	107.33	70.75	189.04
Ta	197.39	250.82	170.68	113.32	74.74	199.09
W	200.25	255.83	172.46	116.88	77.35	205.58
Re	201.39	258.73	172.72	119.90	79.52	210.82
Os	201.51	259.13	172.70	120.71	80.00	211.96
Ir	200.43	255.50	172.89	116.05	76.74	204.16
Pt	197.88	247.84	172.90	104.83	69.43	186.49
Au	193.43	241.49	169.41	106.07	68.87	184.69

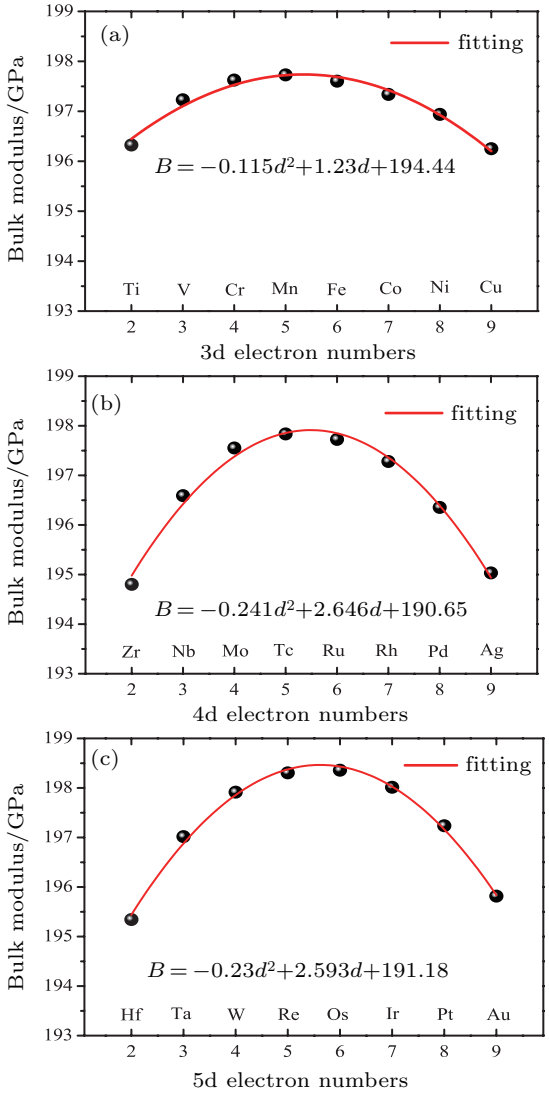


Fig. 1. (color online) Bulk modulus as a fitting function of d electrons for the 3d, 4d and 5d group transition metal elements in the $Ni_{107}X$ systems.

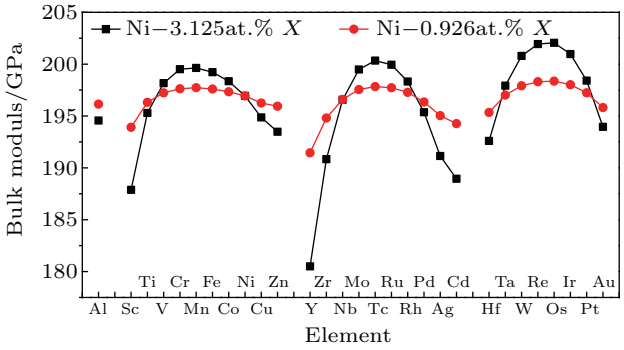


Fig. 2. (color online) Influence of alloying elements on bulk modulus at various concentrations, showing the $Ni_{107}X$ systems with red dots and the $Ni_{31}X$ systems with black dots.

The bulk modulus of an alloy is related to the number of d electrons of the alloying element. Figure 1 shows that the bulk modulus has a parabolic relationship with the number of d electrons. Within the same period, the bulk modulus reaches its maximum when the d electron shell is half full, and is related to the maximum exchange energy. The bulk modulus shows a nearly perfect parabolic behavior, with a maximum at $d = 5$.

In order to explore the relationship between the doping concentration and mechanical properties of the materials, we calculated the bulk modulus of Ni alloyed with 29 elements at concentrations of 0.926%, and 3.125%, corresponding respectively to $Ni_{107}X$ and $Ni_{31}X$ models. The calculated result is shown in Fig. 2. The results show a nearly perfect parabolic behavior for both $Ni_{31}X$ and $Ni_{107}X$ models.

From Fig. 3 we conclude that, assuming a dilute solid solution, there is a linear relationship between bulk modulus and alloying concentration. Using linear regression, we obtained the linear fit coefficient a_i^{B} as follows:

$$B_i^{\gamma}(x_i) = a_i^{\mathrm{B}} x_i + B_0^{\gamma}, \tag{11}$$

where x_i is the alloying concentration, $B_i^{\gamma}(x_i)$ is the γ-phase bulk modulus alloyed with element i, a_i^{B} is the bulk modulus concentration coefficient of element i, and B_0^{γ} is the bulk modulus of pure Ni.

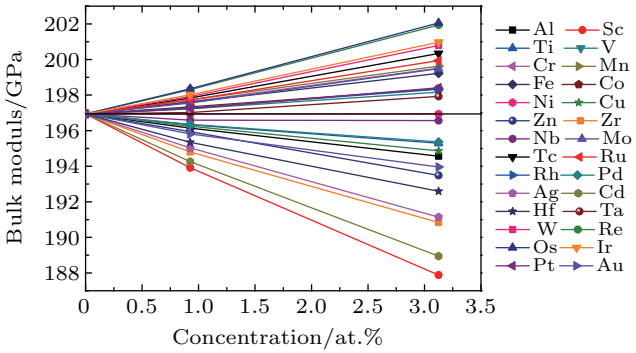


Fig. 3. (color online) The bulk modulus of Ni alloyed with 29 elements at concentrations of 0%, 0.926%, and 3.125%, corresponding respectively to pure Ni, $Ni_{107}X$, and $Ni_{31}X$.

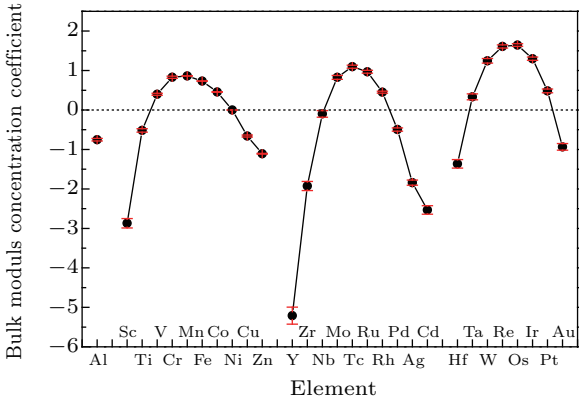


Fig. 4. (color online) The bulk modulus concentration coefficient of various elements (GPa/at.%).

The bulk modulus concentration coefficient can describe how the bulk modulus depends on various alloying concentrations. Figure 4 shows the bulk modulus concentration coefficient of 29 elements. Within given elements, the trend of the bulk modulus concentration coefficient is also parabolic, similar to the trend of the bulk

modulus. The horizontal dashed line in Fig. 4 shows the concentration coefficient of pure Ni is zero, points above dashed line showing strengthening effect and points below it show weakening effect. Based on the concentration coefficient, the alloying elements strengthen the γ-Ni in this order: Os > Re > Ir > W > Tc > Ru > Mn > Cr > Mo > Fe > Pt > Co > Rh > V > Ta > Ni > Nb > Pd > Ti > Cu > Al > Au > Zn > Hf > Ag > Zr > Cd > Sc > Y.

Based on these results, Re, W, Ru, Cr, Mo, Co, Ir, Pt all strengthen the solid solution, and Re and W show the strongest effects. Based on this discussion, we obtain a concentration coefficient of the bulk modulus that affects the mechanical properties of the alloys. We can use the concentration coefficient to get the bulk modulus at any concentration, which helps greatly in designing the alloy composition. To see whether this law applies to other alloys, such as those Co-based, Al-based, or Mg-based alloys, we will study the deeper physical mechanism in future work.

3.1.1. Binding energy of single alloying elements

To explain how adding an alloying element strengthens a system, we must gain detailed and accurate information about how the alloying element affects structural stability. The strength and structural stability of a crystal are closely related to its binding energy. Larger deviation in the absolute value of binding energy from zero indicates greater system stability. The definition of binding energy is

$$E_{\text{binding}} = E_{\text{total}} - \sum_i n_i E_i^{\text{atom}}, \tag{12}$$

where E_{total} is the total energy of the system, n_i is the number of atoms of element i in the system, and E_i^{atom} is the energy of a free atom of element i. The single-atom energy can be calculated using the large lattice cells method from first principles, as shown in Table 3.

Table 3. Free atom energy of elements calculated by first principles (eV).

Element	Atom energy	Element	Atom energy	Element	Atom energy
Sc	–2.10517	Y	–2.1689		
Ti	–2.31967	Zr	–2.11233	Hf	–3.47416
V	–3.56164	Nb	–3.1834	Ta	–3.48725
Cr	–5.48173	Mo	–4.58741	W	–4.53768
Mn	–5.15445	Tc	–3.36609	Re	–4.59875
Fe	–3.39351	Ru	–2.52724	Os	–2.89981
Co	–1.95715	Rh	–1.38302	Ir	–1.5155
Ni	–0.77029	Pd	–1.47216	Pt	–0.55169
Cu	–0.2408	Ag	–0.33771	Au	–0.28341
Zn	–0.16297	Cd	–0.16608		

Figure 5 shows the relationship between the binding energy and the bulk modulus in the $Ni_{31}X$ system. Re, Os, Ir, Tc, Rh, W, Mo, V, Ru, and Pt reduce the binding energy of the system (more negative), making the structure more stable, while improving its elastic properties. Thus, these elements are ideal for strengthening the γ-phase solid solution. Ta, Nb, Ti, and Al make the structure more stable and form the γ' phase. However, Ta and Nb barely improve its elastic properties, and Ti and Al harm its elastic properties. Fe, Co, and Cr barely affect the alloy bonding energy, but increase its bulk modulus. Re, W, Mo, Ru, Cr, Co, Ta, Nb, Ti, and Al are the basic alloying elements in most commercial superalloys. In recent years, some researchers have tried to add Ir and Pt to improve alloys. Elements such as Pd, Cu, Au, Zn, Ag, and Cd, which have a nearly full electron shell, increase the binding energy of the system and decrease its stability, and they do not enhance its elastic properties. Thus, these elements harm the alloy. Also, we found no published alloy compositions that included these elements, indicating that our calculated results reflect the actual design decisions in the literature.

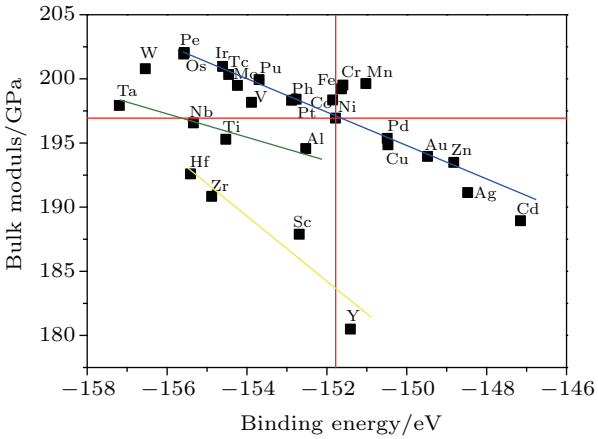


Fig. 5. (color online) Bulk modulus as a function of binding energy in $Ni_{31}X$.

Overall, we did not find a consistent linear relationship between binding energy and bulk modulus, but some of these elements may have an approximately linear relationship, indicating that elements in different parts of the periodic table have different effects on the mechanical properties of their alloys. Various elements affect the system differently in a way related to the electronic structure of the alloying element. The alloying elements can be divided into three groups based on their role.

(i) The elements that form solid solution in the γ phase of the high-temperature alloy, such as Re, Mo, Ru, Co, and Cr, show a negative linear relationship (blue line). W deviates from the blue line and the green line, which may be related to its uniform distribution in two phases. Fe, Cr, Co, and Mn deviate slightly from the blue line, which may be from ignoring spin-induced effects.

(ii) The elements that form γ' phase (Al, Ta, Nb, and Ti) show a negative linear relationship (green line).

(iii) Hf, Zr, and Sc show a negative linear relationship (yellow line).

Combined with the above discussion, solid solution strengthening elements in the γ phase show that the smaller the binding energy, the larger the bulk modulus, that is, the more stable the system, the better its elastic properties.

3.1.2. Influence of alloying elements on bond order

Table 4 and figure 6 summarize the bond order of the vacancy located in the first nearest neighbor of the alloying element.

Table 4. Mayer bond order between alloying elements and Ni in $Ni_{31}X$.

Elements	Bond order	Elements	Bond order	Elements	Bond order
Sc	0.2556	Y	0.1508		
Ti	0.3334	Zr	0.3091	Hf	0.2716
V	0.3754	Nb	0.3519	Ta	0.3597
Cr	0.3507	Mo	0.3772	W	0.4097
Mn	0.3452	Tc	0.3706	Re	0.408
Fe	0.315	Ru	0.3289	Os	0.3737
Co	0.2623	Rh	0.2688	Ir	0.3143
Ni	0.2411	Pd	0.2273	Pt	0.2786
Cu	0.2084	Ag	0.206	Au	0.2486
Zn	0.223	Cd	0.2147		

The interaction between the two atoms increases as the bond order increases. In the γ phase, the bond order increases as follows: W > Re > Mo > V > Os > Tc > Ta > Nb > Cr > Mn > Ti > Ru > Fe > Ir > Zr > Pt > Rh > Hf > Co > Sc > Ni > Au > Pd > Zn > Cd > Cu > Ag > Y. This trend is similar to that of the elastic modulus.

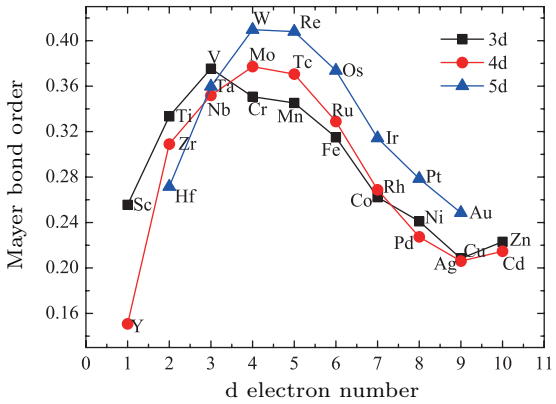


Fig. 6. (color online) Mayer bond order between the alloying elements and Ni in $Ni_{31}X$ systems.

3.1.3. Bader charge analysis

Bader charge analysis[21] was performed for the obtained charge density of Ni31X (X =3d, 4d, and 5d group elements) alloys, as shown in Table 3. The atomic charges were obtained by subtracting the Bader charge from the number of valence electron considered for a particular atom in the density functional theory calculation. Overall, alloying greatly affects the local atomic charge.

Figure 7 shows that Al, Ti, Hf, Ta, W, Re, and Mo have negative Bader charge, indicating that these elements lose electrons. Among these elements, Al has less electrons and losses more electrons than the other elements. Sc, Ti, Y, Zr, Nb, Hf, and Ta are similar to Al. With increasing number of d electrons, Rh, Pd, Ir, and Pt gain electrons. Ru, Cu, and Os gain electrons in an equivalent amount to Ni. We conclude that for elements with less than 8 d electrons, their Bader charge transfer is proportional to their number of d electrons. With more d electrons, the element can gain more charge.

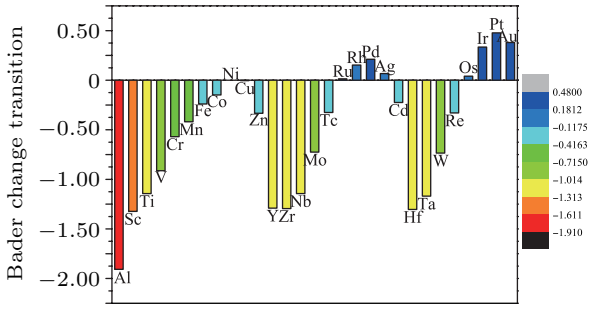


Fig. 7. (color online) Bader charge of various alloying elements (Al, 3d, 4d, 5d).

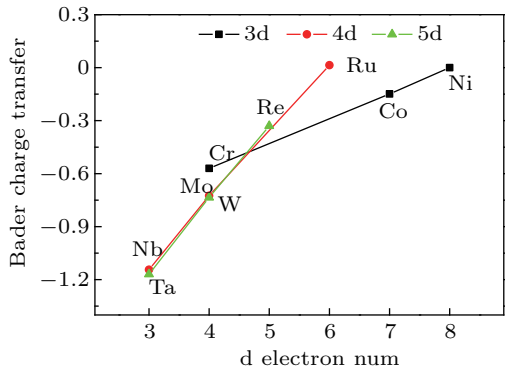


Fig. 8. (color online) Bader charge of 3d (Cr, Co, Ni), 4d (Nb, Mo, Ru), and 5d (Ta, W, Re) elements.

Table 5. Bader charge and Bader charge transfer of alloying elements.

Element	EN^{AR}	Bader charge	Element	EN^{AR}	Bader charge	Element	EN^{AR}	Bader charge
Sc	1.2	–1.35	Y	1.11	–1.23			
Ti	1.32	–1.08	Zr	1.22	–1.34	Hf	1.23	–1.34
V	1.45	–0.81	Nb	1.23	–1.19	Ta	1.33	–1.21
Cr	1.56	–0.62	Mo	1.3	–0.78	W	1.4	–0.76
Mn	1.6	–0.48	Tc	1.36	–0.32	Re	1.46	–0.14
Fe	1.64	–0.33	Ru	1.42	0.12	Os	1.52	0.10
Co	1.7	–0.24	Rh	1.45	0.22	Ir	1.55	0.29
Ni	1.75	0.00	Pd	1.35	0.22	Pt	1.44	0.62
Cu	1.75	0.08	Ag	1.42	0.07	Au	1.42	0.47
Zn	1.66	–0.31	Cd	1.46	–0.20			

Cr, Co, Nb, Mo, Ru, Ta, W, or Re are the elements usually added to Ni-base superalloys. We have independently studied these elements, revealing a perfect linear relationship between the charge transfer and the number of d electrons within a given period. The 4d elements and 5d elements have consistent slopes, indicating that the transition elements in these two periods have similar interaction mechanisms. For example, Nb is similar to Ta, and Mo is similar to W, as shown in Fig. 8.

The Allred–Rochow electronegativity[22] can be found by taking the electrostatic force exerted by the effective nuclear charge Z_{eff} on the valence electron as follows:

$$\chi^{\text{AR}} = \frac{3590 Z_{\text{eff}}}{r_{\text{cov}}^2} + 0.744, \tag{13}$$

where r_{cov} is the covalent radius. Allred and Rochow added certain parameters so this electronegativity would correspond better to Pauling's electronegativity scale.

Among Cr, Co, Ni, Nb, Mo, Ru, Ta, W, and Re, there is a positive linear relationship between charge transfer and number of d electrons. We will discuss the mechanism of this relationship in future work.

Figure 9 shows the linear relationship between the electronegativity of the element and its ability to gain charge. With increasing electronegativity, Bader charge transfer increases, with Pt showing the largest effect. All the elements in the 3d period, except Cu, lose electrons. With more d electrons in the 4d and 5d periods, the ability to gain electrons gradually increases; Ru, Ir, Pt, and other elements with more than six d electrons all gain electrons, except Cd.

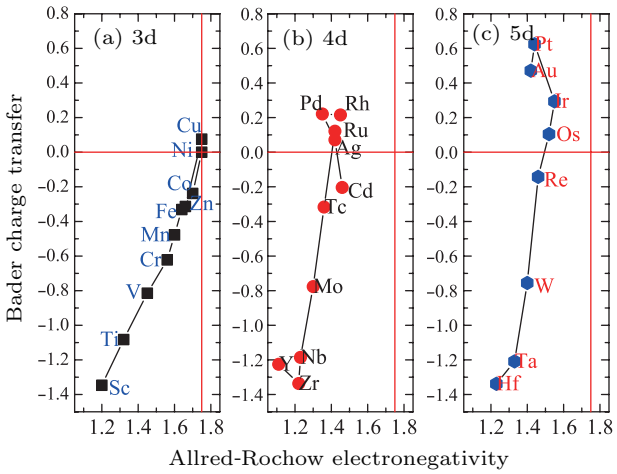


Fig. 9. (color online) The relationship between electronegativity and Bader charge transfer for the 3d, 4d, and 5d transition metal.

3.2. Influence of alloying concentration on the elastic properties of Ni

Our results show that, by alloying with a single element, more than ten alloying elements produced a high-temperature alloy with excellent performance. This has important implications in studying the synergistic effect of adding multiple elements on the mechanical properties, because it is challenging to describe the mechanical properties of such an alloy using a quantitative method.

Most of the alloying elements in the γ-Ni form a disordered solid solution. Assuming a dilute solid solution, we vary the concentration of the alloying element by varying the size of the unit cell. However, the system cannot be infinite because of first-principles computational constraints, so this method is limited to systems over a set range of concentrations.

The disordered configurations of the atoms in the alloys were considered within the special quasi-random structures (SQS) framework,[23,24] which simulates a random solid solution alloy system by using a special quasi-stochastic structure of binary alloys, rather than by constructing supercells. This framework is the most common and successful special random structure used to calculate semiconductors and transition metal alloys. Figure 10 shows the SQS model for 32 atoms alloyed at 6.25% concentration.[25] For an $Ni_{30}X_2$ system, two alloying elements are located in first-nearest-neighbor positions and the symmetry is orthorhombic. An orthorhombic crystal has nine independent elastic constants.

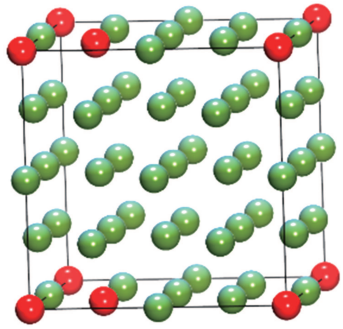


Fig. 10. (color online) Atomic model of $Ni_{30}X_2$, where green balls represent Ni atoms and red balls represent alloying atoms.

From Fig. 11, it is not difficult to find out that the elements with different concentration are similar to those obtained from the single-element model. Re, W, Os, Ir, and other solid solution strengthening element have the strongest enhancing effect and also show a parabolic trend in their respective periods. The maximum value appears when the d shell of electrons is half full. The elemental concentration coefficient is used to predict the bulk modulus of the alloying element with the alloying concentration of 6.25 at.%. The prediction formula is

$$B_{\text{Ni30}X_2}^{\text{Predict}} = B_{\text{Ni}} + a_X c_X = B_{\text{Ni}} + 6.25 a_X^{\gamma}. \tag{14}$$

Using linear regression, we fit the predicted and calculated values to study the relationship between the two elements. The results (Fig. 12) show very high linearity with a slope of 0.9904, and the fit of the regression line to the data has a regression parameter of $R^2 = 0.99626$. This parameter is close to 1, indicating that the regression line fits very well, and the slope is also close to 1, indicating that our prediction formula—a linear function of alloy concentration—is reasonable. Overall, the predicted values are very close to the calculated values.

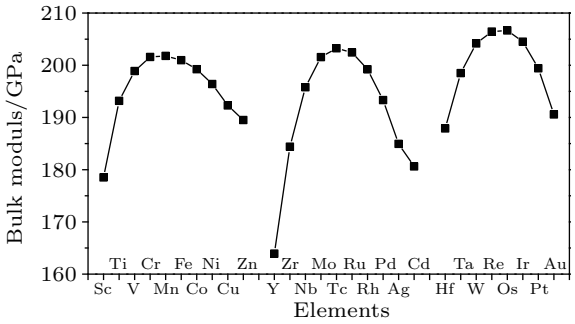


Fig. 11. The bulk modulus of $Ni_{30}X_2$ with various alloying elements.

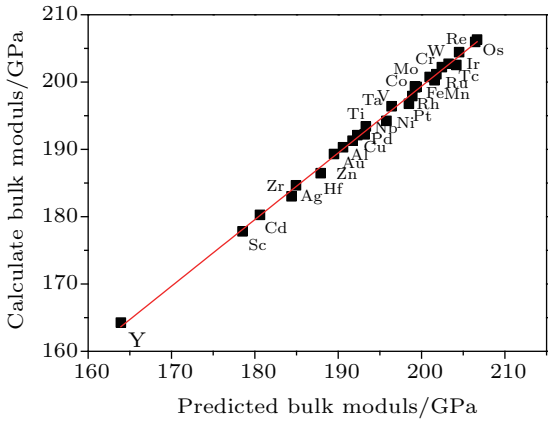


Fig. 12. (color online) The linear relationship between the predicted lattice constant and the calculated bulk modulus in $Ni_{30}X_2$.

To further verify our predictions over a wider range of compositions, we studied the $Ni_{30}XY$ ternary alloy, using a model similar to the model of the binary system. In this model, the two elements occupy the first-nearest-neighbor sites. We studied the synergistic effect of the two elements on the elastic properties of Ni alloys, and then verified that our theoretical predictions in the ternary system are reasonable.

We designed 841 (29×29) models by combining 29 elements. In total, there are 435 inequality systems considering the symmetry (Ni_{30}–X–Y = Ni_{30}–Y–X). These 435 systems contain a combination of binary elements and Ni: Ni_{30}–Ni–X, Ni_{30}–X–X. We used high-throughput job processing to write the relevant procedures, as well as automatic job submission, monitoring, and processing of results. These results are shown in Fig. 13.

The horizontal and vertical axes of Fig. 13 represent the two-part combination $Ni_{30}XY$ of 29 elements (Al, 3d, 4d, 5d), which is a 29×29 matrix with a total of 841 systems. Each square is the matrix element of the elemental combination. The color of the square represents the magnitude of the bulk elastic modulus, gradually increasing from blue to red. The map of combinations shows periodicity, demonstrating that the elastic properties of the alloy largely depend on the combination of elements.

We predict the bulk modulus of $Ni_{30}XY$ based on the bulk elastic modulus concentration factor obtained earlier, and examine the relationship between the predicted and actual values. The prediction formula is

$$B^{\text{Predict}}_{Ni_{30}-X-Y} = B^{\gamma}_0 + a^{\gamma}_x C_x + a^{\gamma}_Y c_Y. \quad (15)$$

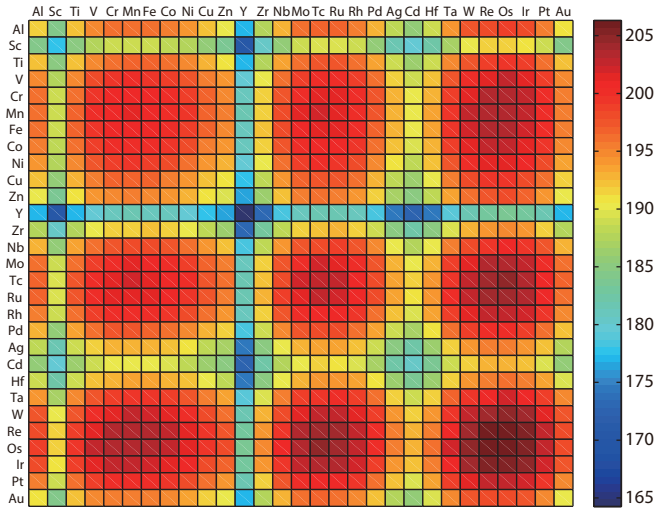


Fig. 13. (color online) Bulk modulus map in Ni_{30}–X–Y.

Figure 14 shows the relationship between the theoretical prediction and the calculated value. We used linear regression to analyze the data, revealing a very good linear relationship between the predicted and calculated values. The resulting slope of the fit is 1.0032, very close to 1. The regression parameter is $R^2 = 0.99431$, indicating that the regression line fits well with the data. This result validates our prediction formula: the bulk modulus of the ternary system still has a linear relationship with the elemental concentration coefficient, within a certain concentration range.

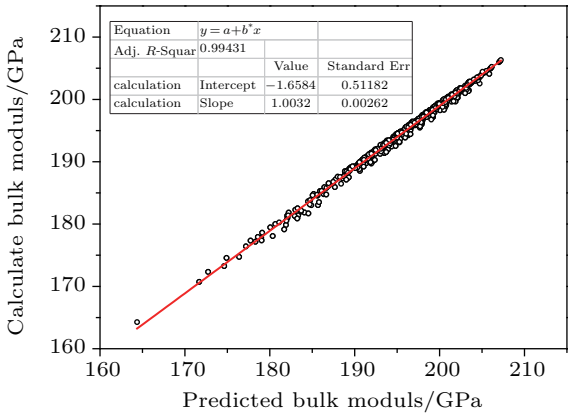


Fig. 14. (color online) Linear relationship between the predicted and calculated bulk modulus in Ni_{30}–X–Y (X, Y = Al and 28 kinds of 3d, 4d, and 5d elements).

3.2.1. Relationship between bulk elastic modulus and other mechanical properties

The brittleness or toughness of a compound can be predicted by its B/G ratio, as proposed by Pugh.[2] The critical B/G is 1.75: generally, a material with a higher B/G (> 1.75) is ductile, while a material with a lower B/G (< 1.75) is brittle. The Poisson's ratio (ν) can also be used to estimate the

brittle or ductile behavior of a material, as ductile materials often have larger ν (> 0.26).

Figures 15 and 16 show the poisson's ratio ν map and shear modulus G map. Analyzing the ν and G between the 29 elements have an obvious periodicity and closely related electronic configuration of the elements. When d-electrons of element close to half full-shell state possess better strengthening effect.

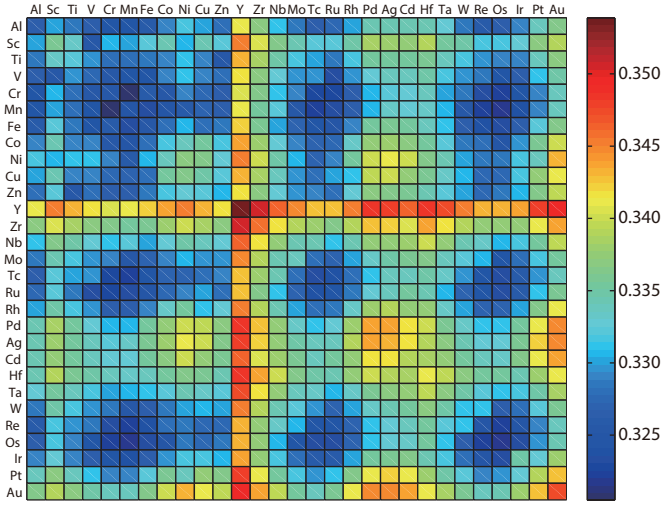


Fig. 15. (color online) Poisson's ratio map of Ni_{30}–X–Y systems.

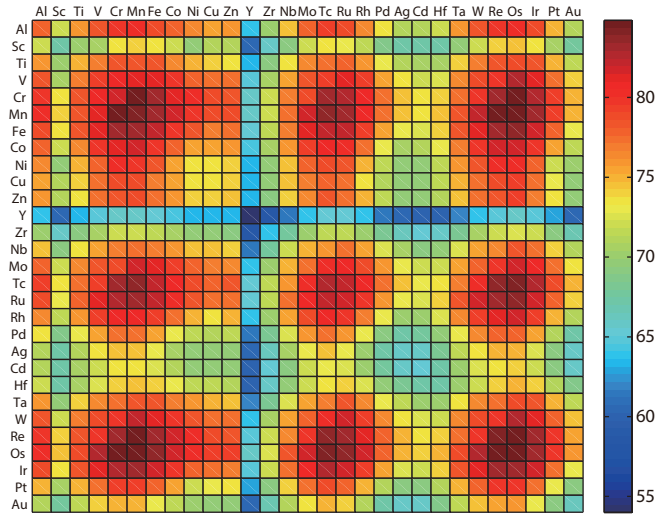


Fig. 16. (color online) Shear modulus map of Ni_{30}–X–Y.

Using linear regression to fit B and G gives a linear regression coefficient of $R^2 = 0.8385$, indicating a positive correlation, as shown in Fig. 17. This relationship also shows that G increases with B, but with a looser correlation. To assess this, we divide the interval by the values of B and G of pure Ni (black line in Fig. 17) into four regions. The interval in the fourth quadrant increases as B increases and G decreases. The figure shows almost no points in the fourth quadrant, where adding alloying elements increases the bulk elastic modulus B and G. According to Pugh's rule, the ductile or brittle nature of a material is closely related to the ratio of its shear modulus G to its bulk elastic modulus B, G/B, and its Poisson's ratio. The larger the G/B or the smaller the Poisson's ratio, the more brittle the material. Based on this rule, we can judge the effect of alloying elements on the toughness or brittleness of the material.

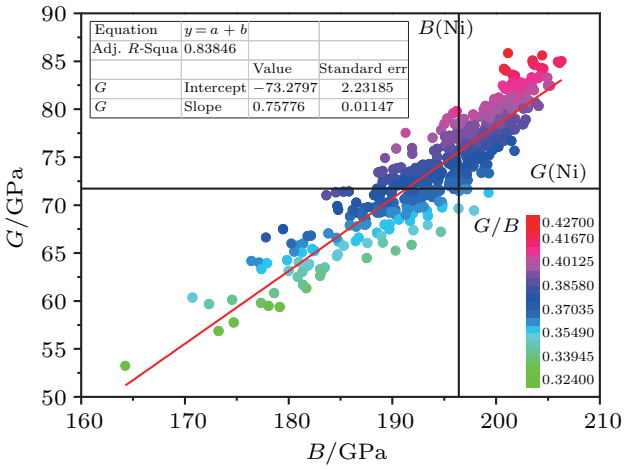


Fig. 17. (color online) The relationship between the bulk modulus B and shear modulus G.

In Fig. 17, G/B is shown by the color of the dot, where red indicates a larger G/B. Shown in this trend, as B increases, G/B will also increase, so the alloy becomes more brittle. This point also appears in the relationship between the modulus and Poisson's ratio: roughly, the Poisson's ratio decreases as B increases, as shown in Fig. 18. The Poisson's ratio is smaller than that of pure Ni in the fourth quadrant, where B is increased, which indicates that adding these alloying elements will increase brittleness. Figure 19 shows a positive correlation between B and E as well as the elastic coefficients C_{11}, C_{12}, and C_{44}, and the relationship between the shear modulus discussed above is similar. As B increases, Young's modulus, C_{11} and C_{44}, will not decrease. C_{12} tends to increase and B will increase.

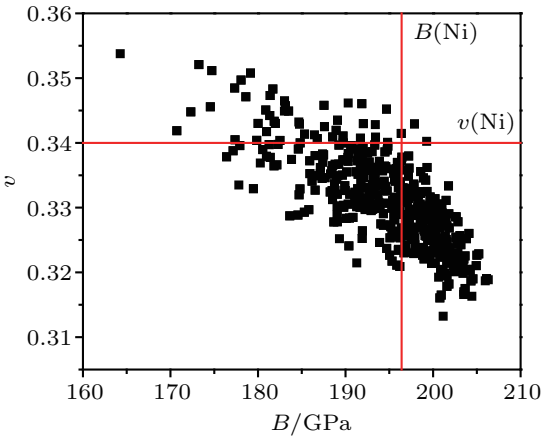


Fig. 18. (color online) Relationship between bulk modulus and Poisson's ratio.

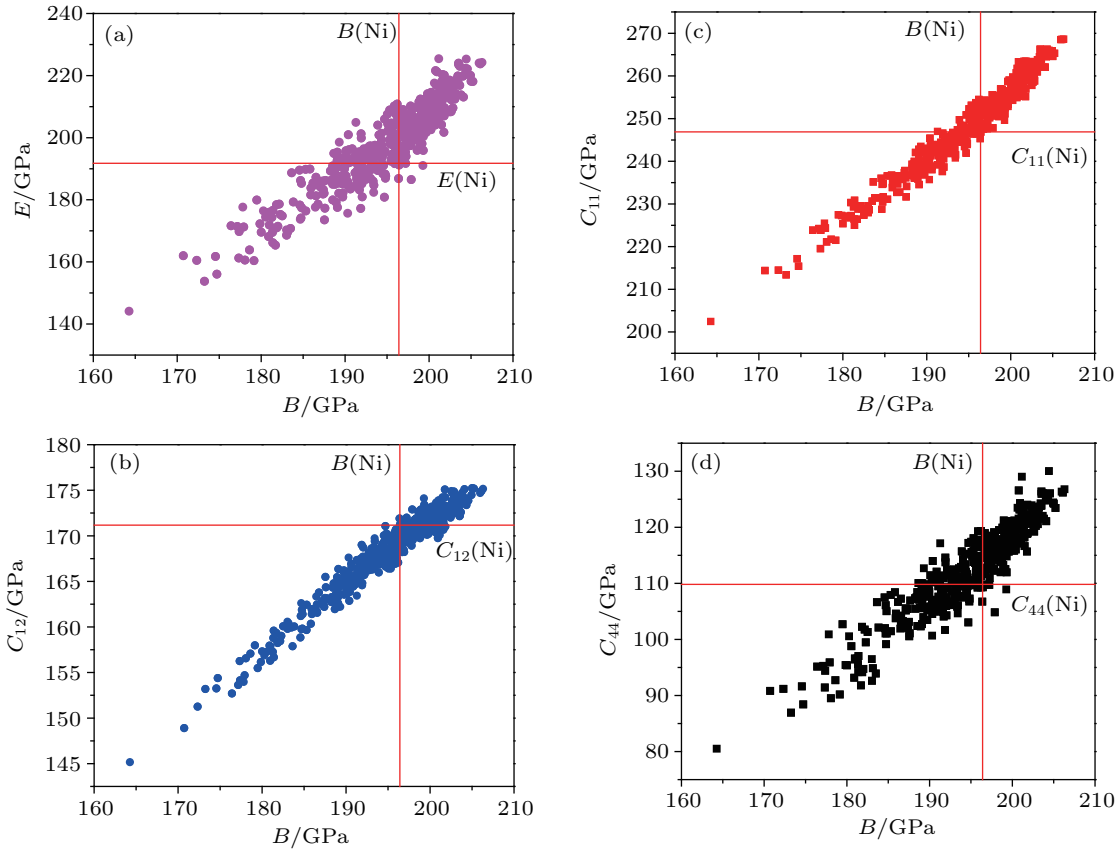


Fig. 19. (color online) Relationship between the bulk modulus and Young's modulus as well as the elastic coefficients C_{11}, C_{12}, C_{44} in $Ni_{30}XY$: (a) B–E, (b) B–C_{11}, (c) B–C_{12}, and (d) B–C_{44}.

3.2.2. Structure stability and bulk modulus

As shown in Fig. 20 of the whole compositional space, alloying elements from different periods have different functions and reflect the complicated synergistic effect between two elements. This result indicates that 5d elements (such as Re and W) improve the stability of the alloy crystal structure more than the 3d and 4d elements do. Additionally, the binding energy is lower at $d = 3, 4, 5, 6, 7$ and helps more to increase the stability of the system.

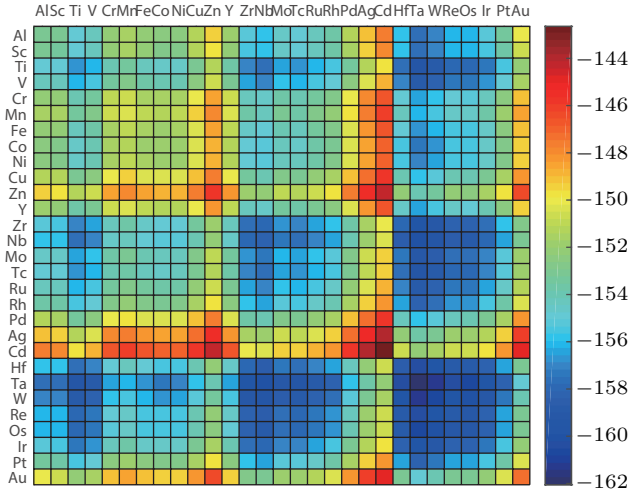


Fig. 20. (color online) Binding energy map of $Ni_{30}XY$.

To study the relationship between binding energy and bulk modulus, we divide the compositions into four regions separated by the binding energies and bulk moduli of pure Ni.

(1) $E_{\text{binding}} < E^{\text{Ni}}_{\text{binding}}$, $B > B^{\text{Ni}}$, increase system stability, increase bulk modulus;

(2) $E_{\text{binding}} > E^{\text{Ni}}_{\text{binding}}$, $B > B^{\text{Ni}}$, decrease system stability, increase bulk modulus;

(3) $E_{\text{binding}} < E^{\text{Ni}}_{\text{binding}}$, $B < B^{\text{Ni}}$, increase system stability, decrease bulk modulus;

(4) $E_{\text{binding}} > E^{\text{Ni}}_{\text{binding}}$, $B < B^{\text{Ni}}$, decrease system stability, decrease bulk modulus.

The light green zone (1) falls within our preferred compositional space for the alloy, while the light blue zone (4) is an unfavorable constituent space. Figure 21 shows that the points in the zone (1) are relatively dense and approximate a linear relationship (shown within the purple oval), which is a ternary system composed of alloying elements. The points in the zone (2) show a few deviations, because systems containing Cr, Fe, and Mn do not account for the spin interactions in calculations. We conclude that in all these alloys, increasing its binding energy and increasing its elastic modulus do not occur at the same time. All the alloying elements that increase the bulk modulus reduce the binding energy of the system. This result shows that the binding energy is a good criterion to judge the effect of alloying elements on the mechanical properties of gold alloys. The smaller the binding energy, the greater the

improvement in mechanical properties.

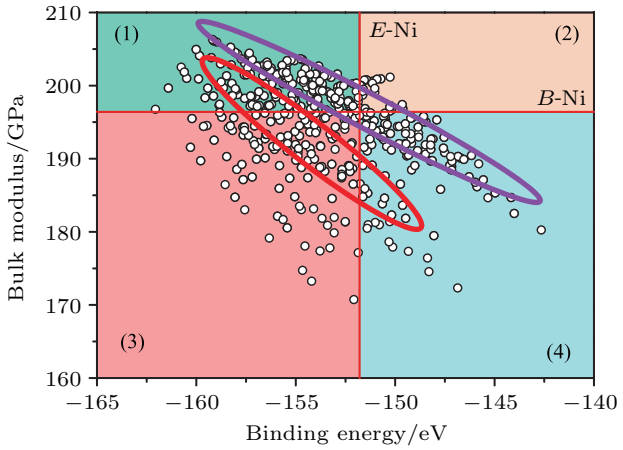


Fig. 21. (color online) Relationship between binding energy and bulk modulus in $Ni_{30}XY$.

3.2.3. Metallic atomic radius and lattice constant

Figure 23 shows the lattice parameter as a function of alloying concentration. Here, the change in lattice parameter can be approximated as a linear function of alloying concentration, and the coefficient of the lattice parameter of the alloying elements in γ-Ni is shown in Fig. 24. The lattice parameter has a parabolic relationship with the number of d electrons. In a given period, the bulk modulus reaches its minimum when the d electron shell is half full. The bulk modulus shows nearly perfect parabolic behavior, with a minimum at $d = 5$ or 6. Adding a refractory element, such as Re, Ru, W, or Mo, considerably increases the lattice parameter; Mn, Fe, and Co are the only elements that decrease the lattice parameter. Thus, co-alloying with different elements at different concentrations should further affect the lattice misfit, improving the high-temperature creep strength of superalloys.

Table 6. The metallic atomic radius of 29 elements and the lattice constant of the $Ni_{107}X$ and $Ni_{31}X$ alloys (Å).

Element	Radius	$Ni_{107}X$	$Ni_{31}X$	Element	Radius	$Ni_{107}X$	$Ni_{31}X$	Element	Radius	$Ni_{107}X$	$Ni_{31}X$
Al	1.43	3.518	3.523	–		–	–	–		–	–
Sc	1.62	3.524	3.543	Y	1.8	3.531	3.565	–		–	–
Ti	1.47	3.520	3.530	Zr	1.6	3.526	3.551	Hf	1.59	3.525	3.547
V	1.34	3.518	3.521	Nb	1.46	3.523	3.541	Ta	1.46	3.523	3.539
Cr	1.28	3.516	3.517	Mo	1.39	3.521	3.532	W	1.39	3.521	3.533
Mn	1.27	3.516	3.515	Tc	1.36	3.520	3.529	Re	1.37	3.520	3.530
Fe	1.26	3.516	3.514	Ru	1.34	3.520	3.528	Os	1.35	3.520	3.529
Co	1.25	3.516	3.515	Rh	1.34	3.520	3.530	Ir	1.355	3.520	3.531
Ni	1.24	3.517	3.517	Pd	1.37	3.521	3.534	Pt	1.385	3.522	3.535
Cu	1.28	3.517	3.520	Ag	1.44	3.523	3.541	Au	1.44	3.524	3.543
Zn	1.34	3.519	3.524	Cd	1.51	3.525	3.547				

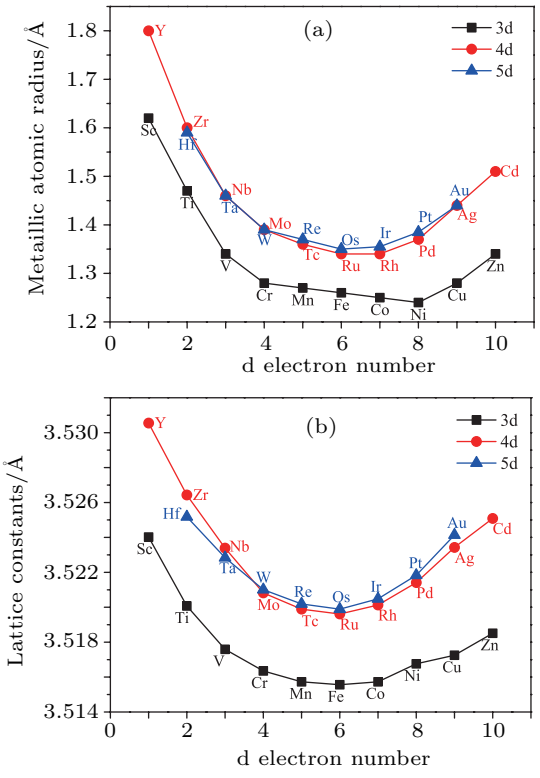


Fig. 22. (color online) (a) Metallic atomic radius and (b) lattice constant as functions of the number of d electrons.

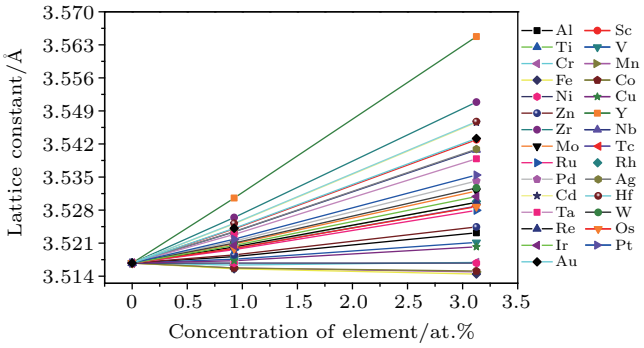


Fig. 23. (color online) Effect of alloying concentration on the lattice parameter of various γ-Ni alloys.

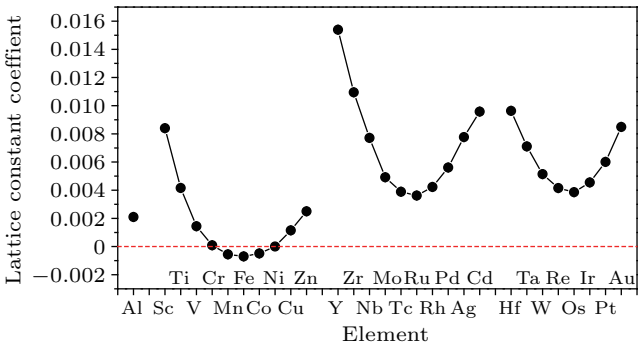


Fig. 24. Coefficient of lattice parameter for alloying elements in γ-Ni.

To verify whether the volume effect of the alloying element on the system in the ternary alloy system is also a linear relationship of concentration, we used a fitting method similar to that of the bulk modulus, as follows:

$$a^{\text{predict}}_{\text{Ni}_{30}-X-Y} = a_0^{\text{Ni}} + b_X^{\gamma} c_X + b_Y^{\gamma} c_Y,$$

where a_0^{Ni} is the lattice constant of pure Ni, b_X^{γ} and b_Y^{γ} are the lattice constant concentration factors of the alloying elements X and Y, respectively, and c_X and c_Y are the concentrations of X and Y, respectively.

The horizontal axis in Fig. 25 is predicted by fitting the concentration coefficient of the lattice constant. The ordinate is calculated from first principles. The predicted value shows a very good linear relationship with the calculated value. Using linear regression, the slope of the fit is 0.99879, which is very close to 1, and the regression parameter is $R^2 = 0.99837$. R^2 is close to 1, so the regression line fits very well, validating the proposed prediction formula. Overall, in the Ni ternary system, the lattice constant still has a linear relationship to the concentration coefficient.

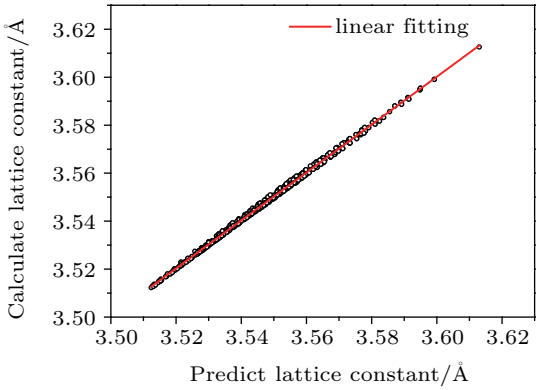


Fig. 25. (color online) The linear relationship between the predicted and calculated lattice constant.

4. Conclusion

We systematically investigated how Al and 28 transition metals affected the elastic properties of γ-Ni. The alloy strengthening was closely related to the electronic structure of the alloying elements. In the model for a single alloying elements, the bulk modulus is related to the number of electrons in the d shell of the alloying element and exhibits a "parabolic" trend over a given period, which can be perfectly fit with a quadratic function and reaches a maximum at a half-full shell of $d = 5$. The alloying elements strengthen γ-Ni in the following order: Os > Re > Ir > W > Tc > Ru > Mn > Cr > Mo > Fe > Pt > Co > Rh > V > Ta > Ni > Nb > Pd > Ti > Cu > Al > Au > Zn > Hf > Ag > Zr > Cd > Sc > Y.

Changing the size of the unit cell also changed the alloying concentration of the element. The bulk modulus had a linear relationship with the alloying concentration. Using linear regression, we fit the bulk modulus concentration coefficients of various alloys. Using a prediction formula, we successfully predicted the concentration coefficient of many test binary and ternary systems: 28 $Ni_{30}X_2$ systems and 435 $Ni_{30}XY$ systems.

Our predictions agreed well with calculated results: the linear regression showed an excellent regression parameter of $R^2 = 0.99431$, validating the relationship between the modulus and alloying concentration. We analyzed the dependence of the bulk modulus and elastic constants (C_{11}, C_{12}, C_{44}), elastic modulus (Young's modulus, shear modulus), and Poisson's ratio of 435 $Ni_{30}XY$ ternary systems, showing that adding an alloy that increases the bulk modulus B will also increase the shear modulus G, Young's modulus E, C_{11}, and C_{44} without increasing the bulk modulus B or decreasing the other parameters. C_{12} is special, because in a system where C_{12} increases, B will increase the modulus. However, B and other mechanical parameters do not have better linear consistency, indicating that the choice of alloying elements will affect more than one parameter. In addition, by calculating the total system combination, we found that all the alloying elements that increase the bulk moduli of all these systems reduced the system binding energy, indicating that the binding energy is also a good criterion for assessing the elastic properties of the alloy. Ni-based alloys showed a negative correlation between the binding energy of the alloying element in the solid solution and the elastic modulus.

We also studied how alloying affected the lattice constants of γ-Ni, revealing a linear relationship between lattice constant and alloying concentration. By using linear regression, we obtained the lattice constant concentration coefficients of various alloying elements. As before, we used the concentration coefficient to predict how adding the alloying element would affect many binary and ternary systems, and the lattice constants of 435 $Ni_{30}XY$ ternary systems were consistent with the calculated results. Linear regression gave an excellent regression parameter of $R^2 = 0.99837$, validating our prediction formula. By assessing different lattice constants of the elements in the two phases, we can predict the mismatch of the alloy, which has very good applications.

Acknowledgment

Simulations were performed using the Explorer 100 cluster system at the Tsinghua National Laboratory for Information Science and Technology, Beijing, China.

References

[1] Reed R C 2006 *The Superalloys: Fundamentals and Applications* (Cambridge: Cambridge University Press)
[2] Pugh S 1954 *Philos. Mag.* **45** 823
[3] Kresse G and Hafner J 1993 *Phys. Rev. B* **48** 13115
[4] Kresse G and Hafner J 1994 *Phys. Rev. B* **49** 14251
[5] Kresse G and Furthmüller J 1996 *Phys. Rev. B* **54** 11169
[6] Kresse G and Furthmüller J 1996 *Comput. Mater. Sci.* **6** 15

[7] Kresse G and Joubert D 1999 *Phys. Rev. B* **59** 1758
[8] Perdew J P, Burke K and Ernzerhof M 1996 *Phys. Rev. Lett.* **77** 3865
[9] Monkhorst H J and Pack J D 1976 *Phys. Rev. B* **13** 5188
[10] Voigt W 1928 *Lehrbuch der kristallphysik: Teubner-Leipzig* (New York: Macmillan)
[11] Reuss A and Angew Z 1929 *Math. Mech.* **9** 55
[12] Hill R 1952 *Proc. Phys. Soc. London* **65** 350
[13] Wang Y J and Wang C Y 2009 *MRS Fall Meeting Symp. FF Proc.*
[14] Wang Y J and Wang C Y 2009 *Chin. Phy. B* **18** 4339
[15] Wang Y J and Wang C Y 2009 *Phil. Mag.* **89** 2935
[16] Wu X X and Wang C Y 2015 *J. Phys.: Condens. Matter* **27** 295401
[17] Shang S L, Wang Y, Kim D E and Liu Z K 2010 *Comput. Mater. Sci.* **47** 1040
[18] Shang S L, Kim D E, Zacherl C L, Wang Y, Du Y and Liu Z K 2012 *J. Appl. Phys.* **112** 053515
[19] Kim D E, Shang S L and Liu Z K 2012 *Acta Mater.* **60** 1846
[20] Kim D E, Shang S L and Liu Z K 2009 *Comput. Mater. Sci.* **47** 254
[21] Bader R F 1990 *Atoms in Molecules-A Quantum Theory* (Oxford: Oxford University Press)
[22] Allred A L and Rochow E G 1958 *J. Inorg. Nucl. Chem.* **5** 264
[23] Zunger A, Wei S H, Ferreira L G and Bernard J E 1990 *Phys. Rev. Lett.* **65** 353
[24] Wei S H, Ferreira L G, Bernard J E and Zunger A 1990 *Phys. Rev. B* **42** 9622
[25] Tian L Y, Hu Q M, Yang R, Zhao J J, Börje Johansson and Levente Vitos 2015 *J. Phys.: Condens. Matter* **27** 315702